Aalborg Universitet

A study of dynamic behaviour performance of DCDC boost converter used in the photovoltaic system

Snani, Hamza; Amarouayache, M; Bouzid, Aissa; Lashab, Abderezak; Bounechba, Hadjer

A study of dynamic behaviour performance of DC/DC boost converter used in the photovoltaic system

H. Snani, M. Amarouayache, A. Bouzid, A. Lashab, H. Bounechba

Laboratory of Electrical Engineering, Department of Electrical Engineering
Constantine 1 University, 25000 Constantine, Algeria
E-mail: hmz_snani@yahoo.fr, amarouayachemohamed@yahoo.fr, you.bouzid@yahoo.fr
lashab_abderezak@hotmail.com, hadjerbounechba@yahoo.com

Abstract—**As the continuously fluctuation of the operating point due to the permanent research of maximum power point which the photovoltaic source can product, the dynamic behaviour of the used DC/DC converter -adopted to realize the maximum power point tracking- will be disturbed at all time. For the aim to design an efficient photovoltaic system, the dynamic behaviour of the converter is studied based on the damping factor and the natural frequency of the system. As an example, the system under study is composed with a photovoltaic module connected to an equivalent resistive load through a DC/DC boost converter, assuming that this last one has been controlled with a direct method of maximum power point tracking. The results of analytical studies allow having an overview about the dynamic behaviour performance of the used DC/DC converter for the aim to implement a prompt maximum power point tracking algorithm.**

Keywords—*Photovoltaic (PV) cell; DC/DC boost converter; maximum power point (MPP); maximum power point tracker (MPPT); damping factor (ξ); natural frequency (ω_0).*

I. INTRODUCTION

Solar photovoltaic is envisaged to be a popular source of renewable energy due to several advantages, notably low operational cost, almost maintenance free and environmentally friendly [1].

A PV module under uniform irradiation exhibits an *I-V* characteristic with a unique point, called the maximum power point (MPP), where the module produces maximum output power [2]. The amount of the produced power depends on the operating point, which is the intersection between the *I-V* characteristics of both PV module and the connected load. It is known that the efficiency of the PV cells is low (14 to 16% for the monocrystalline Si), therefore, it is necessary to operate at the MPP at all time whatever the climatic conditions and the connected load are.

The DC/DC converter is usually used for realizing the MPPT function through the injection on its principal switching power component, the right pulse width control signal (*d*) using a MPPT algorithm.

In cloudy days, the solar irradiation can be random and very volatile (which can have a rate of 100 W/m²/s [3]). Consequently most of the MPPT algorithms, among them the perturb and observe (P&O) which can be confused due to the fact that it is not able to distinguish the variations of the PV module output power caused by the duty cycle modulation from those ones caused by the irradiance variation [2], hence a judicious optimization of an efficient MPPT algorithm must take place. Among the optimized parameters, the sampling time (T_s) which is strongly depends on the dynamic behavior of the used DC/DC converter.

In the case where there is no effect of the connected load on the output PV voltage (v_{pv}), the knowledge of the transfer function of the control to v_{pv} ($F_{vpv, d}$) is enough for designing a stable and robust system to face different fluctuations of MPP.

This work is focusing on the variation of both ξ and ω_0 of the system (see fig. 1) which their formulas are extracted from ($F_{vpv, d}$) of an approximated second order system. The interval variation of both ξ and ω_0 as well as the system operating point changes, allows us having an overview about the dynamic behaviour performance of the used DC/DC converter for the aim to implement a prompt maximum power point tracking algorithm.

The paper is organized as follows. The PV cell based on the two diode model is presented in section II. The transfer function ($F_{vpv, d}$) and its simplification to a second order are developed in section III. Criteria of the transient response are given in section IV. The results of analytical studies and discussions are shown in section V. Finally section VI is devoted to conclusion.
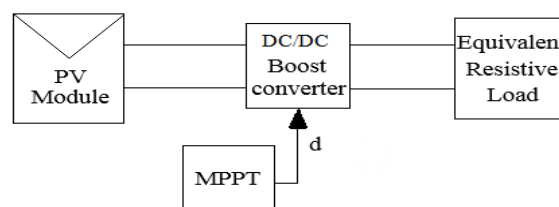

Fig. 1. The considered system under study.

II. Moddeling of the PV cell

The development of PV system has demanded the need of simulation tools capable of handling mathematical simulations [4]. Due to its good representation of the output *I-V* characteristic, under different values of irradiation and temperature, the model of two diode is taken, it is defined as indicated in fig. 2, by an electrical source associated to two diodes (D1, D2) and two resistances (Rs, Rsh). The diode (D1) represent the semi-conductor behaviour, which constitute the PV cells, and the other diode (D2) is a compliment of the first one that is used for more accurate curves under different levels of irradiation, when Rs and Rsh represent the different contact losses and the leakage current to the ground through the PV cell respectively.
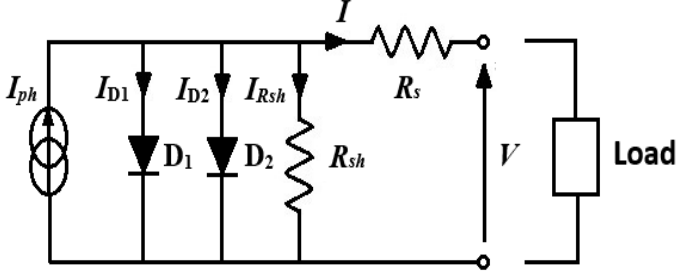

Fig. 2. The two diode model of the PV cell.

Fig. 3, shows the obtained electrical characteristics of STP080S-12/Bb module from SUNTCH Company under some solar irradiation and temperature combinations.
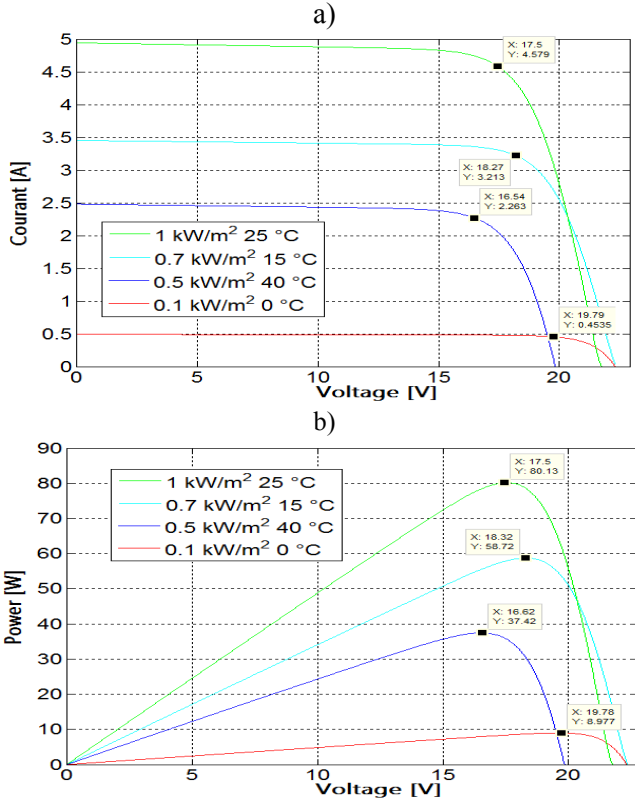

Fig. 3. Output characteristics of the used PV module under some combinations of the solar irradiation and temperature; a) *I-V* curves b) *P-V* curves.

III. Moddeling of boost converter

A. Small signal model

The DC/DC boost topology presents a good efficiency in the PV application especially its continuous input courant, which is useful for extracting all the amount of power as the PV module can product. Many DC/DC topologies have been used in this type of application [5][6]. The used equivalent circuit of the DC/DC boost converter (dotted line in fig. 4) is constituted with a passive components (L, C_{pv} and C_o), which are sized away to have a continuous conduction mode (CCM). The formulas used are found in references [7][8]. The switches S and D are in general a transistor (IGBT) and a diode respectively.

The input and output of the converter are connected respectively to PV module -which is modelled with a dynamic resistance (r_{pv}) that define the ratio between the instantaneous voltage and courant of the PV module- and to an equivalent resistive load (R_o), when the input and the output voltages are the instantaneous values of the PV voltage ($v_{pv}(t)$) and capacitor voltage ($v_o(t)$) respectively.
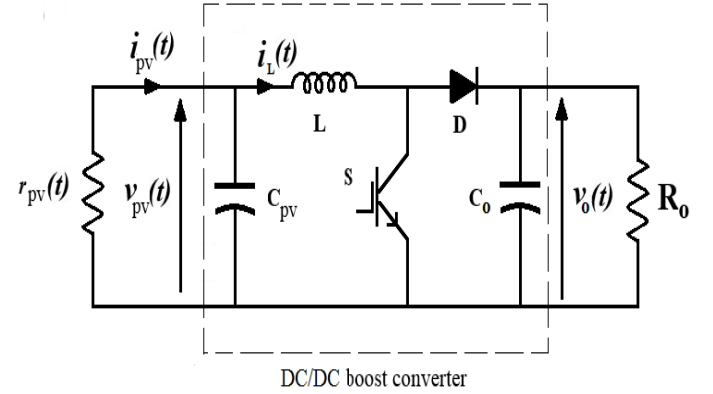

DC/DC boost converter

Fig. 4. The equivalent circuit of the considered system

In power electronic, the switches' number (N) determines the number of the elementary configurations as 2^N. In the pulse width modulation (PWM) control, and for the CCM, there are two stable configurations which appear every switching period (T_{sw}) *1) i.e.* when S is switched-on and D is switched-off in the interval time $0 \leq t_{on} \leq dT_{sw}$, *2) i.e.* when S is switched-off and D is switched-on in the interval time $dT_{sw} \leq t_{off} \leq T_{sw}$ where *d* is the duty cycle ($d = t_{on}/T_{sw}$).

The state variables according to these configurations are:

$$\begin{cases} \dfrac{dv_{pv}}{dt} = -\dfrac{v_{pv}}{C_{pv}r_{pv}} - \dfrac{i_L}{C_{pv}} \\ \dfrac{di_L}{dt} = \dfrac{v_{pv}}{L} - (1-s)\dfrac{v_o}{L} \\ \dfrac{dv_o}{dt} = -\dfrac{v_o}{C_oR_o} + (1-s)\dfrac{i_L}{C_o} \end{cases} \quad (1)$$

Where *s* is time-dependent switching variable, defined as:

$$s(t) = \begin{cases} 1 & \text{For S is switched} - \text{on} \\ 0 & \text{For S is switched} - \text{off} \end{cases} \quad (2)$$

Based on (1) the small signal averaged state-space model is obtained as shown in (3) at the bottom of this page, where the variables with a hat are small AC variations about the equilibrium operating point, V_{pvE} is the equilibrium value of the output PV voltage and r_{pv} is a dynamic resistance that define the ratio - $\widehat{v_{pv}}/\widehat{\iota_{pv}}$. Other symbols in (3) refer to Fig. 4.

B. Transfer function and the obtained second order system

By applying the Laplace transform to (3), the small signal control to module voltage transfer function ($F_{vpv,\,d}$) is obtained as shown in (4) at the bottom of this page, where s here is the Laplace variable.

According to control theory of linear systems, the transient response and dynamic behavior of (4) strongly depends on the nature of the poles' denominator ($D(s)$). We note that this last one is a third degree polynomial.

To facilitate the study of the converters' dynamic behavior, the idea is to get a comparable system to a second order in the general form:

$$D(s) = s^2 + 2\omega_0 \xi s + \omega_0^2 \qquad (5)$$

Where the natural frequency ω_0 characterizes the time response of the system (i.e., the good variations of ω_0 provide a fast transient response) since the damping factor ξ characterizes the oscillation during the transient response (i.e., the good variations of ξ provide a well damped system).

The pair of complex conjugate poles then characterize the system of second order are:

$$s_{1,2} = -\omega_0\xi \pm j\omega_0\sqrt{1-\xi^2} \qquad (\text{If } 0 \leq \xi < 1) \qquad (6)$$

The characteristic polynomial wanted, take the following form:

$$D(s) = (s^2 + 2\xi\omega_0 s + \omega_0^2)(s - s_r) \qquad (7)$$

Equation (7) accepts three poles, at least one is real (s_r), the other two poles ($s_{1,2}$) are either real (if the discriminate $\Delta_{D(s)} > 0$) or complex conjugate (if $\Delta_{D(s)} < 0$). Therefore, to obtain a second order system, we must put s_r as far as possible

in the left half complex plane and place the two complex poles ($s_{1,2}$) the closest possible to the imaginary axis (see Fig. 5), In this case s_r has a negligible influence on the transient response.
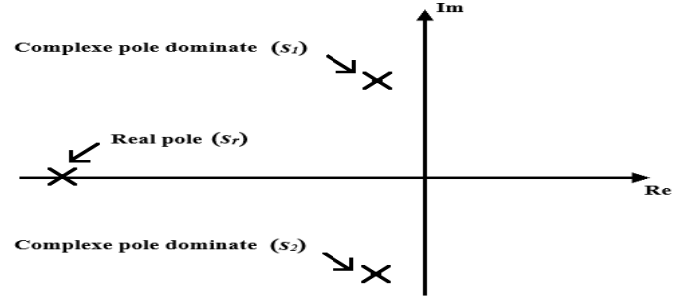

Fig. 5. Dominate poles' placement of a second order system.

Therefore, we can write the second condition:

$$|Re(s_r)| \gg |Re(s_{1,2})| \qquad (8)$$

The denominator $D(s)$ of (4) is a third degree polynomial of the general form:

$$D(s) = d_3 s^3 + d_2 s^2 + d_1 s + d_0 \qquad (9)$$

Applying (8) on (7, 9), we obtain requirements imposed on the coefficients (d_0, d_1, d_2, d_3) of (9) for getting a second order system dominate. We obtained the following system of equations:

$$\begin{cases} s_r = -d_2 \\ \omega_0 = \sqrt{\dfrac{d_0}{d_2}} \\ \xi = \dfrac{d_1 d_2 - d_0}{\sqrt{4 d_0 d_2^3}} \end{cases} \qquad (10)$$

Based on (10), the values of L, C_{pv}, and C_o will be chose (we respect the CCM). The dynamic resistance r_{pv} defines the operating point on the characteristic I-V and it depends on the temperature and solar irradiance. This resistance takes big values if the solar irradiation takes small values and *vice versa*.

$$\frac{d}{dt}\begin{pmatrix} \widehat{v_{PV}} \\ \iota_L \\ v_o \end{pmatrix} = \begin{bmatrix} -1/(C_{pv}rpv) & -1/C_{pv} & 0 \\ 1/L & 0 & -(1-d)/L \\ 0 & (1-d)/C_o & -1/(C_o R_o) \end{bmatrix} \cdot \begin{pmatrix} \widehat{v_{PV}} \\ \iota_L \\ v_o \end{pmatrix} + \begin{bmatrix} 0 \\ \frac{V_{pvE}}{L(1-d)} \\ \frac{-V_{pvE}}{C_o rpv} \end{bmatrix} \cdot (\hat{d}) \qquad (3)$$

$$F_{vpv,\,d}(s) = \frac{\dfrac{-V_{pvE}}{LC_{pv}(1-d)}s - \dfrac{2V_{pvE}(1-d)}{LC_{pv}C_o rpv}}{s^3 + \left[\dfrac{1}{rpv}\left(\dfrac{(1-d)^2}{C_o}+\dfrac{1}{C_{pv}}\right)\right]s^2 + \left[\dfrac{(1-d)^2}{C_o}\left(\dfrac{1}{C_{pv}rpv^2}+\dfrac{1}{L}\right)+\dfrac{1}{LC_{pv}}\right]s + \dfrac{2(1-d)^2}{LC_{pv}C_o rpv}} \qquad (4)$$

The second parameter (d) defines the transformation ratio between the input and the output of the converter; it gives the level voltage of the load connected.

The first step for having a second order system is to have discriminate $\Delta_{D(S)} < 0$ whatever the variations in irradiation and temperature (the interval variation of r_{pv}) and whatever the variation in load (The interval of duty cycle $0 \leq d < 1$). This condition decides the first interval dimensioning the elements (L, C_{pv}, and C_o).

The following figure shows the variations of the discriminant ($\Delta_{D(S)}$) in the predefined intervals of r_{pv} and d for our converter topology.
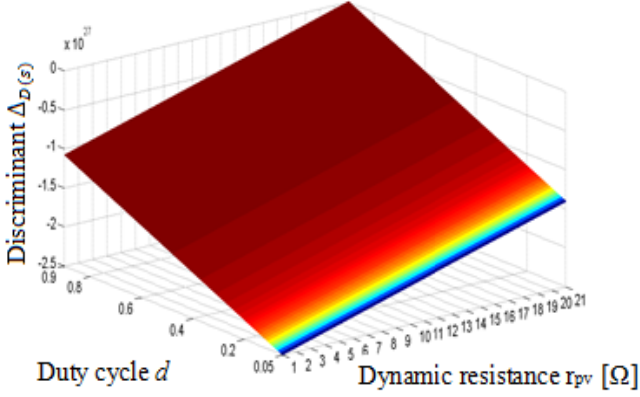

Fig. 6. Variations of discriminant-boost topology.

Obviously, $\Delta_{D(S)}$ is negative whatever the values of r_{pv} and d used in the design of the elements of storage. So the first condition is verified.

The second condition (8) which is to having a very real pole away from the imaginary axis. This condition determines the sub-range of L, C_{pv}, and C_o. Solving (10) gives a relationship between L, C_{pv}, and C_o for having a real pole non-dominant.

Fig. 7, shows the placement of poles and zeros of the transfer function $F_{vpv, d}(s)$. For example if $r_{pv} = 20 \ [\Omega]$ and $d=0.5$ the placement of the real pole (s_r) is as far from the two conjugate poles ($s_{1,2}$) that can neglect its influence on the transient response. So in this case, the system can be presented by the transfer function as shown in Fig. 8.
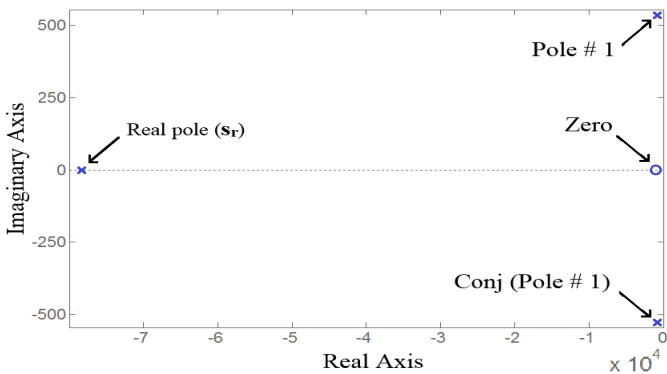

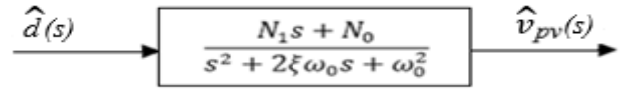Fig. 7. Placement of poles and zeros of the boost transfer function ($F_{vpv, d}(s)$).

Fig. 8. Transfer function of a second order system.

Formulas (11, 12) describe the dependence of ξ and ω_0 on the system parameters, so we will study the variations of these two parameters according to the variations of both r_{pv} and d.

$$\xi = \frac{C_{pv}(L + C_{pv}r_{pv}^2)(1-d)^4 + LC_o(1-d)^2 + C_o^2 r_{pv}^2}{2r_{pv}(1-d)\sqrt{2L[C_{pv}(1-d)^2 + C_o]^3}}$$

(11)

$$\omega_0 = (1-d)\sqrt{\frac{2}{L(C_{pv}(1-d)^2 + C_o)}}$$

(12)

IV. CRETERIA OF THE TRANSIENT RESPONSE

In a second order system, the factors (ξ, ω_0) characterize the step transient response (fig. 9).
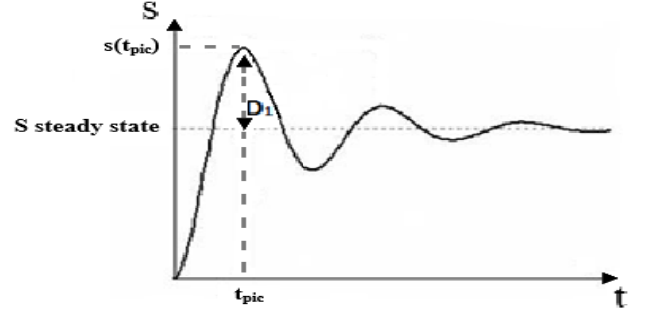

Fig. 9. Transient response to a step.

This transient response is characterized by a first overtake (D_1), reflecting the degree of damping of the system and the first peak time (t_{pic}), reflecting the rapid transient. It is generally desired to obtain a fast transient and well damped, therefore obtained a MPPT fast and less oscillate.

The first overtake (D_1) and time to peak (t_{pic}) of the transient are directly related to ξ and ω_0 by the following relationships:

$$t_{pic} = \pi/(\omega_0\sqrt{1-\xi^2})$$

(13)

$$D_1 = 100e^{-\pi\xi/\sqrt{1-\xi^2}}$$

(14)

V. RESULTS OF THE ANALYTICAL STUDY

In the following as it indicated in Fig. 8, we will show the variation influence of both ξ and ω_0 on v_{pv} as this last one should be characterized to be a well damped and fast when the transient response for the aim to implement a more efficient MPPT algorithm.

A. Discussion about the damping factor (ξ)

We know according to control theory of linear systems that a good sizing of ξ (≈ 0.703) minimizes the system's oscillations in the transitional phase by decreasing D_1 which implies a will damped system so the corresponding losses will be reduced when the MPPT action. According to (11), the obtained analytical form of ξ depend on both d and r_{pv}. Fig. 10, shows its variations.
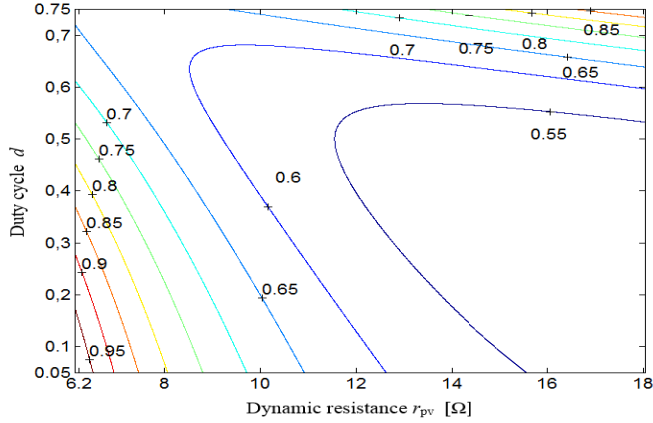

Fig. 10. Damping factor ξ versus some combinations of d and $r$pv.

B. Discussion about the natural frequency (ω_0)

A good sizing of ω_0 reduces the system's time response that implies fast MPPT reactions.

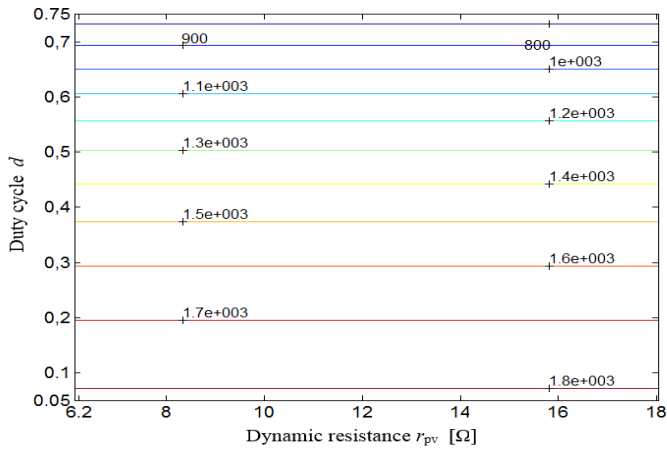Based on (12), it is found that the analytical form of ω_0 depends only on d. Fig. 11, shows its variations.

Fig. 11. Natural frequency ω_0 [rad/s] versus some combinations of d and $r$pv.

C. Criteria of the transient response

The criteria of the transient response (t_{pic}, D_1) are indirectly related to the variations of both r_{pv} and d through the variation of ξ and ω_0.

- **The first peak time (t_{pic})**

The formula (13) of $tpic$ depends on both ξ and ω_0 so its variations are indirectly influenced by the variations of r_{pv} and d. Fig.12, shows a specified variation interval of both r_{pv} and d because for the rest of their intervals, t_{pic} takes values less than 0.02 [s]. These obtained values are translated that ω_0 has more influence than ξ on t_{pic} variations, which implies that d is the more important parameter that influences the time to the first overtake of the transient response.
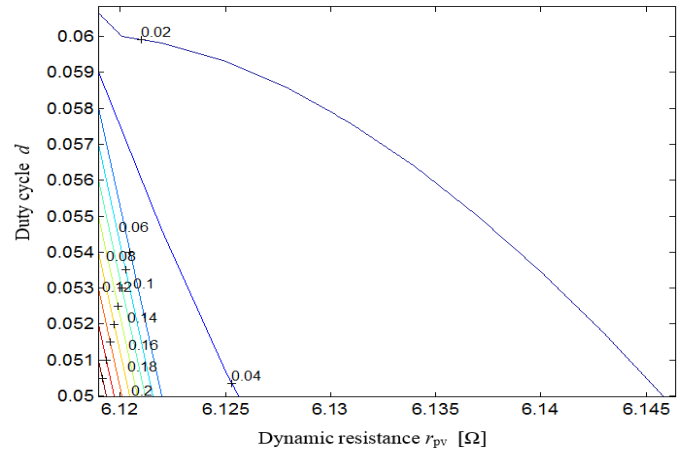

Fig. 12. First peak time t_{pic} [s] versus some combinations of d and $r$pv.

- **The first overtake (D_1)**

According to (14), the first overtake (D_1) depends only on ξ which means that the two parameters r_{pv} and d have an influence on its variations, fig. 13, shows these variations.
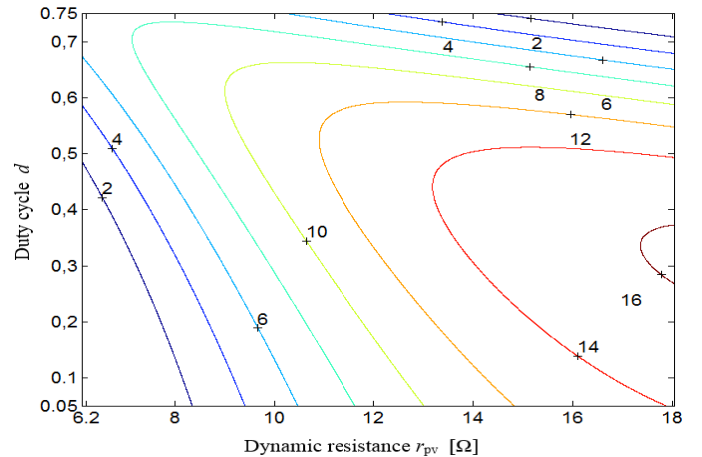

Fig. 13. First overtake D_1 (%) versus some combinations of d and $r$pv.

VI. CONCLUSION

In this paper we have presented a PV system that is constituted with a PV module and an equivalent resistive load, which are connected together using DC/DC boost converter. The transfer function ($F_{vpv,\,d}$) is obtained and its mathematical simplification is applicable for other DC/DC topologies in the case when we want to select which topology dynamic behavior performance is the best one.

The results of analytical studies based on ξ and ω_0 of the obtained second order system, allowed us to take an overview about the transient response behaviour of the output PV voltage according to different operating conditions by studying

its first overtake D_1 and time to peak t_{pic}, for the aim to implement an efficient MPPT algorithm.

REFERENCES

[1] I. Kashif, S. Zainal, M. Amjad, and S. Mekhilef, "An Improved Particle Swarm Optimization (PSO)–Based MPPT for PV With reduced Steady-state Oscillation," IEEE Trans. Power Electron., vol. 27, no. 8, August 2012.

[2] N. Femia, G. Petrone, G.Spagnuolo, and M. Vitelli, "Optimization of perturb and observe maximum power point tracking method," IEEE Trans. Power Electron., vol. 20, no. 4, July 2005.

[3] R. Bründlinger, N. Henze, H. Häberlin, B. Burger, A. Bergmann, F. Baumgartner, prEN 50530 – The New European Standar For Performance Charactirisation of PV Inverters," 24th European Photovoltaic Solar Energy Conf., Hamburg, Germany, September 2009.

[4] S. Bal, A. Anurag, and B. Chitti Babu, "Comparative analysis of mathematical modeling of photo-voltaic (PV) array," IEEE INDICON 2012, Int. Conf., Cochin, December 2012.

[5] A. M. Noman, K. E. Addoweesh, and H. M. Mashaly, "Simulation and Hardware Implementation of the MPPT Techniques Using Buck Boost Converter," IEEE 27th Canadian Conf. Elect. Comput. Eng. (CCECE), May 2014.

[6] A. Safari, and S. Mekhilef, "Simulation and Hardware Implementation of Incremental Conductance MPPT With Direct Control Method Using Cuk Converter," IEEE Trans. Ind. Electron., vol. 58, no. 4, April 2011.

[7] R. N. Tripathi, A. Singh, and M. Badoni, "A MATLAB-Simulink-Based Solar Photovoltaic Array (SPVA) Module with MPPT," Emerging Trends in Communication, Control, Signal Processing & Computing Applications (C2SPCA), 2013 Int. Conf. on, October 2013.

[8] W. Xiao, N. Ozog, and W. G. Dunford, "Topology Study of Photovoltaic Interface for Maximum Power Point Tracking," IEEE Trans. Ind. Electron., vol. 54, no. 3, June 2007.